Virtual Electrodes by Current Steering in Retinal Prostheses

Gerald Dumm[1,2], James B. Fallon[1,3], Chris E. Williams[1,3] and Mohit N. Shivdasani[1,3,*]

[1]Bionics Institute, East Melbourne, VIC-3002, AUSTRALIA

[2]Lübeck University of Applied Sciences, 23562 Lübeck, GERMANY

[3]Medical Bionics Department, The University of Melbourne, East Melbourne, VIC-3002, AUSTRALIA

*Corresponding Author:

Dr. Mohit N. Shivdasani

Bionics Institute, 384-388 Albert Street, East Melbourne, VIC – 3002, AUSTRALIA

Email: mshivdasani@bionicsinstitute.org

Word Count: 4335

Grant Information:

This work was supported by the Australian Research Council through its Special Research Initiative in Bionic Vision Science and Technology awarded to Bionic Vision Australia, the Bertalli Family Foundation to the Bionics Institute, and a project grant from the National Health and Medical Research Council, Australia (Project#1063093). The Bionics Institute wishes to acknowledge the support it receives from the Victorian Government through its Operational Infrastructure Program.

Abstract

Purpose: Retinal prostheses are an approved treatment for vision restoration in retinal degenerative diseases; however, present implants have limited resolution and simply increasing the number of electrodes is limited by design issues. In cochlear implants, virtual electrodes can be created by simultaneous stimulation of adjacent physical electrodes (current steering). The present study assessed whether this type of current steering can be adapted for retinal implants.

Methods: Suprachoroidal electrode arrays were implanted in four normally-sighted cat eyes. Electrode pairs were driven simultaneously at different current levels and current ratios. Multiunit spiking activity in the visual cortex was recorded. Spike distribution across channels enabled generation of cortical activation maps and calculation of centroid positions. For each current configuration, centroid shifts between two virtual electrodes were compared to shifts obtained from physical electrode stimulation.

Results: Using current steering, virtual electrodes with different cortical activation maps could be created. Cortical centroids were found to shift as a function of the current ratio used for virtual electrodes and were similar to the centroid shifts seen when using physical electrodes. In addition, the cortical response to stimulation of a physical electrode could be reproduced by applying current steering to electrodes on either side of the physical electrode.

Conclusions: These results suggest that current steering can alter activation patterns in the visual cortex and could enhance visual perception in retinal implants by eliciting phosphene percepts intermediate between those elicited by physical electrodes. These results inform development of new electrode arrays that can take advantage of current steering.

Introduction

One of the leading causes of blindness is the degeneration of the retina due to a loss of photoreceptors caused by diseases such as retinitis pigmentosa (RP)[1]. The prevalence rate for RP is about one in 4000 which results in more than one million people worldwide who are blinded by this disease[2]. Although there are several therapies being investigated, retinal prostheses remain the only approved treatment for RP[3]. Retinal prostheses aim to restore vision by electrically stimulating the surviving neurons in the inner retina. This is realized by an implantable electrode array which is placed at either one of four locations: epiretinal[4-6], subretinal[7, 8], suprachoroidal[9, 10] and trans-scleral[11, 12]. With the presently available designs, it is possible to regain orientation and mobility of patients to a certain degree[8, 13] and in some patients even the ability to perform spatio-motor tasks[14] and letter and word reading[15] are possible. Although these results are very promising, more advanced levels of visual perception like sentence reading and face recognition which require higher spatial resolution are still out of reach for most patients[3, 16]. Hence there is a demand for technologies that can improve the spatial resolution of retinal implants, particularly when the electrode arrays are located hundreds of microns away from the target neurons, for example with the suprachoroidal approach. One strategy is to merely increase the number of physical electrodes which in turn will increase the number of available “pixels”. However, this approach involves engineering and safety challenges[16].

Current steering describes numerous stimulation paradigms which are applied in modern neuroprosthetics. In general, current steering refers to the effect of simultaneous stimulation of several electrodes on the overall electric field which is formed by overlapping of individual electrode fields. In neural stimulation, current steering is either used for focusing the current, thus narrowing the area of tissue excited, or for redirecting the current to excite different tissue[17]. In the scope of this study, only the latter application will be addressed.

Figure 1 shows the principle of the simplest form of current steering where simultaneous current versus a remote return is applied to an electrode pair on a one-dimensional electrode array to create an intermediate "virtual electrode". When equal current is applied to a pair of electrodes the resultant field peaks at a location mid-way between both electrodes (Fig.1A). When a different current ratio is applied, the peak of the resulting electric field shifts towards the electrode with the higher current (Fig. 1B). Thus the volume of tissue in between the two physical electrodes can be preferentially stimulated. This form of current steering has been successfully used in cochlear implants to produce virtual electrodes that elicit pitch perceptions intermediate to those produced when stimulating physical electrodes. In fact, several studies have shown that it is possible to create on average 4-7 such virtual electrodes between two adjacent physical electrodes in the cochlea[17]. Although a similar form of current steering using electrode pairs has been proposed for the retina when placing the electrode array epiretinally[18], the degree to which current steering is useful for other more distant electrode locations like the suprachoroidal placement, and when using a stimulating electrode array that is clinically relevant, is unknown.

As a first step towards determining whether current steering using electrode pairs can be usefully applied in suprachoroidal retinal implants, we assessed if it was possible to alter the patterns of evoked activity in the visual cortex by stimulating a pair of suprachoroidal retinal electrodes with different current ratios. A successful implementation of current steering in retinal implants could lead to an increase in effective resolution without an increase in the number of physical electrodes, by producing intermediate phosphene perceptions to those produced by physical electrode stimulation.

Materials and Methods

The procedures for this study were approved by the Animal Research Ethics Committee of the Royal Victorian Eye & Ear Hospital and they complied with the "Australian code of practice for the care and use of animals for scientific purposes" (7th edition 2004), the "Principles of laboratory animal care" (NIH publication No. 85–23, revised 1985), and the ARVO Statement for the Use of Animals in Ophthalmic and Vision Research. The surgical techniques, electrode arrays and general procedures have been described in detail previously[19, 20], and so will only be briefly described here.

Surgery

Animals were anesthetized using ketamine (Troy Labs, Australia; 20mg/kg, intramuscular) and xylazil (Troy Labs, Australia; 2mg/kg, subcutaneous), and maintained using a continuous intravenous infusion of sodium pentobarbitone (Troy Labs, Australia; 60mg/kg/hr). Core temperature was maintained at 37±1°C. During the study, the eyes were protected against dehydration with hypromellose gel (GenTeal, Novartis Pharmaceuticals, Australia). Fluid replacement was provided by continuous intravenous infusion of compound sodium lactate solution (Hartmann's solution, 2ml/kg/hr). Respiration rate, CO_2 levels and blood pressure were monitored throughout the experiment. Dexamethasone (Troy Labs, Australia; 0.1mg/kg, intramuscular) was administered for the prophylaxis of brain edema, plus amoxycillin-clavulanate suspension (Clavulox, Pfizer, Italy; 10mg/kg, subcutaneous) as an antibiotic every 24 hours. The experiments were typically conducted over two to three days, after which the animal was terminated.

One eye in each of four normally-sighted adult cats (weighting 2.9 – 5.5kg) was implanted with a clinical grade array in the suprachoroidal space. A lateral canthotomy was performed, followed

by a full-thickness scleral incision 5mm posterior and parallel to the limbus. A pocket was opened between the sclera and choroid and the electrode array was inserted into this pocket and advanced 17mm posteriorly. Effort was made to place the tip of the array underneath the area centralis as the distance of electrodes to the area centralis has an important influence on evoking cortical responses[19].

Suprachoroidal Electrode Array

The design of the suprachoroidal array used for the experiments was similar to what has been applied in previous work[20]. The array consisted of 21 platinum electrodes (600µm diameter) on a 19×8mm silicone substrate. The electrodes were arranged in a hexagonal pattern with a centre-centre spacing of 1mm. Two additional return electrodes with a larger diameter (Ø = 2mm) were located distal to the stimulating electrodes.

Experimental Setup

After implantation, the animal was transferred to an electrically shielded room and placed in a stereotaxic frame (David Kopf Instruments, Tujunga, CA). A craniotomy was performed to expose the visual cortex. A large surface area platinum ball electrode (1.5mm diameter) was used in order to assess the location with the lowest threshold evoked potential for placement of the 60-channel (6x10) recording electrode array (Blackrock Microsystems, Salt Lake City, UT)[19, 21, 22]. The recording array sampled a cortical space area of 2mm in the medio-lateral and 3.6mm in caudo-rostral direction. The penetration depth was approximately 1mm. Multi-unit cortical recordings (band-pass filtered from 0.1 – 7500Hz) were made using the Cerebus system (Blackrock Microsystems, Salt Lake City, UT).

Simultaneous Stimulation for Current Steering

Pairs of electrodes on the suprachoroidal array were stimulated by a custom built constant current source stimulator routed via a cross-point switch matrix[23] that delivered cathodic first biphasic charge-balanced waveforms against a monopolar return electrode. Stimulation pulses had a pulse width of 500μs, an interphase gap of 25μs and a repetition rate of 1Hz. The current between the electrodes in each pair was split according to the following equation 1:

$$I_a = R * I_t \quad (1)$$

where I_a represented the current on the first electrode of the pair and I_t the total current. The variable R (current ratio) was varied between 0 and 1 (0.1 steps) and determined the proportion of current which was allocated to the first electrode. The remaining current was delivered to the second electrode of the pair according to following equation 2:

$$I_b = I_t - I_a \quad (2)$$

where I_b represented the current for the second electrode. Thus current steering was applied for intermediate current ratios (R = 0.1 to 0.9) whereas single electrode stimulation was applied for the extreme current ratios (R = 0 or 1 respectively). The total current amplitude (I_t) was randomized between 0 and 1.5mA (equating to a maximum charge density of 300μC.cm^{-2}) with increments of 50μA (31 different levels). A set of ten repetitions were presented for each current level and current ratio on a given electrode pair. A total of 32 electrode pairs across the four animals were stimulated within this study. The physical distances between the chosen electrodes for each pair were 1mm (13 pairs), 1.7mm (4 pairs), 2mm (6 pairs), 2.6mm (5 pairs) or 3mm (4 pairs).

Data Analyses

Data were cleaned offline as per methods outlined in previous studies[19, 21, 22] and analyzed by using custom scripts in IgorPro (Wavemetrics, Lake Oswego, OR). Artefacts were removed and multiunit spikes (bandpass filtered, 0.3 – 5kHz) were detected and time-stamped when signal exceeded 4.2 times the root mean square value.

Steering Tuning Curves for Single Channels

Figure 2A shows an example of a recorded signal from one recording channel in response to stimulation. Average spike rates across 10 repetitions were analyzed in the first 20ms from stimulus onset (Figure 2B) at each current level to obtain a current-level versus spike-rate input–output function and a sigmoid curve was fitted (Figure 2C). The threshold current was defined as the current amplitude where the sigmoid curve reached 50% of its maximum saturated spike rate[21, 22]. Recording channels were analyzed by plotting average spike rates on a contour plot with the total current amplitude on the x-axis and the current ratio on the y-axis (Figure 2D). By joining the thresholds for each cortical site to each applied current ratio a steering tuning curve was computed. Only channels where at least one current amplitude and ratio combination elicited an average of 2 spikes per repetition or higher were included. Steering tuning curves with the lowest threshold for intermediate current ratios (R = 0.1 to 0.9) indicated that these recording channels preferred steered current as opposed to current only applied to one of the physical electrodes in the pair (R = 0 or 1).

Cortical Spatial Maps and Centroid Shift

For each current ratio, a cortical spatial map was generated by plotting the spike rate across all 60 recording channels at the threshold current of the best cortical electrode (BCE; defined as the

186 recording channel with the lowest threshold for that ratio[21]). Spike rates were normalized to the
187 maximum spike rate of each recording site across all measurements (Figure 3A). The centroid of
188 activity for each map was defined as the spike-count-weighted center of mass across all
189 channels[24]. Centroids for all current ratios of one electrode pair were plotted on a single cortical
190 map to assess the shift between centroids as a function of current ratio (Figure 3B).
191
192 ***Cortical Selectivity***
193 As a measure of the spread of cortical activation, a cortical selectivity value was calculated for
194 each spatial map generated at the current level required to reach 90% of the maximum spike rate
195 on the BCE, according to the method described by Cicione et al[21]. The cortical selectivity for
196 each current ratio applied to each pair of retinal electrodes, represented the degree of the drop in
197 spike rate as a function of the distance from the BCE. The drop in spike rate was fitted using an
198 exponential function and the inverse tau used to quantify the cortical selectivity. Cortical
199 selectivity was compared across current ratios for all electrode pairs.

Results

Steering Tuning Curves for Single Channels

A total of 931 recording channels were analyzed in response to stimulation of 32 electrode pairs. In 8% of the channels, the lowest threshold on the steering tuning curve was found when using an intermediate current ratio indicating that current steering was more effective than single electrode stimulation in activating that recording channel (Figure 2D). In the remaining channels the lowest threshold was found when using single electrode stimulation (i.e. for the extreme current ratios R=0 or R=1).

Cortical Spatial Maps and Centroid Shifts

To quantify centroid shifts between each current ratio applied, the distance between every pair of centroids in the cortex was calculated in mm according to the difference between their corresponding current ratios (ΔR). It was expected that higher ΔR values would result in larger centroid shifts with maximum shifts occurring when $\Delta R = 1$ (i.e. difference between centroid positions when stimulating the two physical electrodes in isolation). Each ΔR value was expressed as a virtual distance in the retina (in mm) by multiplying it by the physical distance separating the two electrodes in the pair. Therefore, when current steering was applied to two electrodes that were physically 1mm apart, a ΔR value of 0.2 would result in a virtual distance of 0.2mm, whereas the same ΔR value for a 2mm physical electrode separation would result in a virtual distance of 0.4mm. All virtual distances were rounded to the nearest 0.1mm. To assess the variability in estimating centroid positions from each cortical spatial map, the centroid shifts seen as a result of repeated single electrode stimulation were also estimated and plotted against a retinal distance of 0mm.

Figure 4A shows the mean cortical centroid shifts as a function of both virtual and physical distances using data from all 32 retinal electrode pairs. Regression lines were fitted to the raw data and showed significant ($p < 0.001$) positive correlation coefficients (Pearson's correlation[25]) both when using virtual electrodes ($r^2 = 0.14$, Slope = 0.287mm cortical shift per mm retinal distance) and when using single electrodes only ($r^2 = 0.5$, Slope = 0.255mm cortical shift per mm retinal distance). A general linear model on centroid shifts, with the factor set as electrode type (physical or virtual) and the co-variate set as distance, showed that centroid shifts were significantly dependent on the retinal distance ($p < 0.001$) but not on whether they were a result of using virtual electrodes or physical electrodes ($p = 0.529$). While physical and virtual shifts in the retina resulted in similar centroid shifts in the visual cortex as seen in Figure 4A, the only distance for which cortical centroid shifts from physical as well as virtual electrodes could be directly compared was 1mm (Figure 4B). A t-test showed that there was no significant difference in the centroid shift between physical electrodes and virtual electrodes at a retinal distance of 1mm ($p = 0.272$).

Cortical Selectivity

Figure 5A shows cortical spatial maps at the current required to reach 90% of the maximum spike rate on the BCE, generated using current steering on a pair of retinal electrodes with the R-value set to 0.5 as well when one of the physical electrodes in the pair was stimulated on its own. The BCE (channel with the lowest threshold, black asterisks in Figure 5A) was the same regardless of using single electrode stimulation or current steering. The drop in spike rate as a function of the distance from the BCE and corresponding inverse tau values of the exponential fits (cortical selectivity) were found to be similar for both modes of stimulation (Figure 5B).

Figure 6 compares the inverse tau values for all data collected in this study across the different current ratios applied. A one-way ANOVA comparing cortical selectivity across the different R-values and for all electrode pairs used for stimulation, showed no significant difference in cortical selectivity ($p = 0.776$) between physical (R-value = 0 or 1) or virtual (R-values between 0.1 – 0.9) electrodes.

Discussion

The aim of this study was to assess if current steering, through simultaneous stimulation of a pair of physical suprachoroidal electrodes, could create virtual electrodes by preferentially activating areas of the retina that lie intermediate to the physical electrodes. We assessed the efficacy of current steering by analyzing data on individual recording channels as well as spatial activation maps across all recording channels in the cortex. We found that a small percentage of individual recording channels showed preference for a steered virtual electrode compared to a physical electrode in terms of requiring a lower threshold of activation. We also demonstrated that the centroid of spatial activation across the cortex could be shifted by varying the current ratio, without affecting the spread of activation.

While our results showed that only a small percentage of individual cortical recording channels had a lower threshold for a virtual electrode as opposed to the majority responding with a lower threshold to a physical electrode, this may have been confounded by the relative position of each physical retinal electrode to the location of area centralis. We have previously shown that cortical channels tend to respond with the lowest thresholds to retinal electrodes that are closer to area centralis[19]. In all the electrode pairs analyzed, one of the physical electrodes was always closer to the area centralis than the other electrode in the pair; hence the likelihood of paired stimulation giving the lowest threshold was small. Furthermore, the odds of having individual channels from our recording set receiving projections from only areas in between physical electrodes were much lower than the odds of retino-cortical projections originating from areas directly beneath or outside the physical electrodes. Therefore, we also examined cortical spatial activation patterns and estimated the centroid of activation across all recording channels to assess the effectiveness of current steering.

The results of analyzing cortical activity maps showed that it was possible to shift the centroid of cortical spike activation by using current steering in the retina on electrode pairs over a range of retinal distances. Generally, larger changes in proportions of current and larger retinal distances (virtual and physical) resulted in larger centroid shifts in the cortex. Moreover, we found no differences in cortical spread of activation between virtual and physical electrodes, which one might have expected if simply a larger area of the retina was being stimulated through an electrode pair compared to the area stimulated by a single electrode. This makes it more likely that the centroid shifts seen in the cortex were a result of localized activation of intermediate areas of the retina that lie in between physical stimulating electrodes as opposed to widespread activation across the two stimulating electrodes.

Based on our results, it is expected that current steering will enable the creation of virtual electrodes in a clinical setting, which would elicit phosphene percepts intermediate to those elicited by stimulating single electrodes. At this stage, the number of possible virtual electrodes obtainable clinically is difficult to estimate from our data, however even with one virtual electrode between each adjacent pair of physical electrodes, the overall number of available pixels would be doubled. It has been shown cochlear implant patients can get on average between 4-7 virtual pitch channels between each pair of physical electrodes[17], but the total number of available channels could be estimated to be as high as 451 using only 12 physical electrodes[26]. Of course for a retinal prosthesis, numerous other factors such as electrode size, pulse parameters, proximity of the electrode to excitable tissue, as well as individual phosphene characteristics (shape, size etc.) will also play an important role in determining the overall resolution.

It was also possible to mimic the centroid location of cortical activation when stimulating physical electrodes, by applying current steering to an electrode pair with a larger spatial distance. For example by using electrode pairs with a spatial distance of 2mm one could create,

using current steering with an R-value of 0.5, a virtual electrode whose position would be 1mm from both electrodes of the pair. Future design of electrode arrays could take advantage of this possibility by spreading electrodes further apart on the array and using current steering to activate intermediate locations. Ultimately this may enable patients to have a wider visual field without a loss in resolution which could significantly improve orientation and mobility. This is of even higher importance when keeping in mind that present commercial retinal implants provide visual fields of only up to 15-20 degrees[8, 13]. Furthermore, current steering could also be used in order to overcome electrode failures (e.g. broken wires) by simultaneous stimulating surrounding electrodes and creating a virtual electrode at the same position as the faulty electrode. Hence a loss in resolution could be avoided.

Limitations of the current study

The present study was performed by implanting normally-sighted eyes. However, a previous study performing suprachoroidal stimulation in a blind animal model showed that threshold values and the activated areas in the superior colliculus were approximately doubled compared to the normally-sighted model[27]. These results emphasize the need to investigate the findings of this study in a blind animal model, although direct testing in patients would provide more concrete evidence of current steering.

Although the results of this study suggest that the resolution of retinal implants could be increased by current steering, certain aspects of its impact on visual restoration remain unclear. While cochlear implant patients are able to get additional pitch information from virtual electrodes, a study assessing the effects of current steering on speech performance[28] has shown that these additional virtual channels do not provide a significant improvement with speech recognition. For retinal implants this may suggest that while generation of additional intermediate

phosphenes may be possible with current steering, it remains unclear whether this will have any impact on visual performance outcomes such as visual acuity. Another question which needs to be addressed is the influence of phosphene overlap on current steering. In the cases of significantly overlapping phosphenes from single electrode stimulation of adjacent electrodes, current steering on an electrode pair would likely provide no additional advantages. However, the use of current focusing techniques to minimize retinal current spread in combination with current steering might be able to overcome this problem. Also, while electrode pairs with different spatial distances were used in this study, based on our results it was not possible to conclusively determine the limit of electrode pitch for effective current steering. In addition, as the method of current steering described in this study will always require pairs of physical electrodes to elicit phosphenes, during this time these physical electrodes will not be available for eliciting their own phosphenes. This may limit the rate at which phosphenes can be presented to the visual system, particularly when using high frame rates. While high frame rates of 50-60Hz have been desirable to avoid flicker perception and convey a quickly changing visual scene, realistic frame rates used in present commercial devices are in the order of 6-8Hz[8, 29], mainly because of the problems found with fading of phosphenes[30]. At these slower frame rates, there should be sufficient time available to interleave stimulation of physical and virtual electrodes within a given video frame by using a short inter-pulse interval. In such situations however, the overall frame rate will also depend on the stimulus parameters used (pulse width, interphase gap and pulse rate per electrode), the time required for charge recovery through electrode shorting, and the number of phosphenes required to be elicited in each video frame. These questions require additional investigation which would best be conducted in the form of psychophysical experiments in retinal prosthesis recipients. Lastly, as one of the next logical steps, two-dimensional current steering should be investigated. Within the present study, current was only divided between two

electrodes while using more than two electrodes during simultaneous stimulation could result in additional virtual electrodes whose positions may not be constrained any longer to a linear intermediate space between an electrode pair. Two-dimensional current steering might offer an even more enhanced boost in resolution for retinal prostheses.

Conclusions

The present study provides first *in vivo* proof of principle that current steering on a pair of stimulating electrodes may be beneficial for retinal implants in terms of being able to create virtual electrodes that produce different activation patterns in the cortex. Beneficial effects of current steering were observed in a small number of cortical recording channels as well as a shift of cortical activity centroids was demonstrated with varying current proportions between electrodes. Mimicking of physical electrodes and generation of additional intermediate virtual electrodes may be possible using current steering between two physical electrodes. It remains to be investigated whether the present results can be reproduced in blind animals and enhanced by applying two-dimensional current steering. Finally, the question whether ultimately virtual electrodes and intermediate phosphenes can be evoked by current steering in blind patients, and whether these phosphenes could indeed improve patient performance, needs to be addressed in human trials.

Figure Legends

Figure 1: The concept of current steering using electrode pairs.

The electric fields expected from single electrode stimulation (E_5 with solid and E_6 with dotted line), and simultaneous stimulation of two adjacent electrodes (dashed line) are shown. Currents on each electrode are represented by the relative height of triangles overlaying the electrode sites. (A) Dashed line represents cumulative electric field for E_5 and E_6 each stimulated with 50% of the total current. (B) Dashed line represents cumulative electric field when E_5 is stimulated using 30% and E_6 is stimulated using 70% of the total current.

Figure 2: Generation of steering tuning curves

(A) Spike recordings on a single cortical recording channel in response to current steering on an electrode pair using a total current level of 1.5mA and an R-value of 0.7. A stimulus artifact (red asterisk) occurred at time zero followed by a burst of spikes within the first 20ms post-stimulus onset. (B) Peri-stimulus time histogram (1ms bin width) for the recording channel in panel A across all current levels used with an R-value of 0.7. (C) Spike count (after artifact removal) in the first 20ms post-stimulus onset plotted against total current level and fitted using a sigmoid curve. (D) Spike activity on the same recording channel in response to current steering using all current levels and current ratios. The total current level is depicted on the x-axis and current ratios are depicted on the y-axis. A steering tuning curve for the threshold current values was appended as a white line. The threshold for this recording channel was lowest when using an R-value of 0.8.

Figure 3: Spatial activation maps and centroid determination

(A) Cortical spatial maps obtained when applying current steering to a pair of retinal electrodes

(only current ratios between 0.3 and 0.7 are shown). A gradual rostral shift of the cortical activity with increasing current ratio is recognizable along with clear shift of the centroids (white asterisks). The dotted box in the leftmost panel represents the reduced area represented in panel B to show the centroid positions for each R-value. (B) The positions of the centroids of cortical activity (marked using x) are depicted on a map for each of the R-values in panel A. Note that axes have been readjusted and do not cover the whole range for x and y-coordinates. C = Caudal, R = Rostral, M = Medial, L = Lateral

Figure 4: Cortical centroid shift for physical and virtual electrode distances

(A) Data for all electrode pairs were combined in order to compare virtual with physical electrode distances. R-square values of calculated regression lines showed a significant correlation between electrode distance and centroid shift. Note: Regression analysis was applied to the scatter plot and not to the mean values (individual data points not shown). (B) Centroid shifts evoked by physical and virtual electrodes with 1mm distance are compared. No significant difference was found indicating the ability of current steering to mimic physical electrodes by applying current steering to either side. Error bars indicate standard error.

Figure 5: Measurement of cortical selectivity

(A) Cortical spatial maps at the current level required to elicit 90% of maximum spike rate on the BCE when stimulating a steered pair of electrodes using an R-value of 0.5 (right) and when stimulating one of the physical electrodes of the pair (left). Black asterisks denote the BCE. (B) Normalized spike rate as a function of the distance from the BCE. Spike rates were normalized to each channel's own maximum spike rate. Data points were fitted with a decaying exponential and the inverse tau value used as a measure of cortical selectivity[21].

Figure 6: Cortical selectivity as a function of R-value

Data from all pairs analyzed (n = 32) showed no significant difference in cortical selectivity (inverse tau) when using current steering on a pair of electrodes (R = 0.1 – 0.9) compared to when using single electrode stimulation (R = 0 or 1). Error bars indicate standard error.

Acknowledgements

The authors thank Owen Burns and Vanessa Maxim for manufacturing of the electrodes, as well as Alexia Saunders and Michelle McPhedran for animal and technical assistance. Also, thanks to Mark Harrison, Austin Mueller and Patrick Thien for stimulator design, construction and software implementation; to Felix Aplin, Rosemary Cicione and Ronald Leung for assistance with data collection; and Joel Villalobos for data analysis suggestions.

References

1. Humayun MS, de Juan E, Jr. Artificial vision. *Eye*. 1998;12 (Pt 3b):605-607.

2. Hartong DT, Berson EL, Dryja TP. Retinitis pigmentosa. *Lancet*. 2006;368:1795-1809.

3. Shepherd RK, Shivdasani MN, Nayagam DA, Williams CE, Blamey PJ. Visual prostheses for the blind. *Trends Biotechnol*. 2013;31:562-571.

4. Ahuja AK, Yeoh J, Dorn JD et al. Factors affecting perceptual threshold in argus ii retinal prosthesis subjects. *Transl Vis Sci Technol*. 2013;2:1.

5. Keseru M, Feucht M, Bornfeld N et al. Acute electrical stimulation of the human retina with an epiretinal electrode array. *Acta Ophthalmol*. 2012;90:e1-8.

6. Klauke S, Goertz M, Rein S et al. Stimulation with a wireless intraocular epiretinal implant elicits visual percepts in blind humans: Results from stimulation tests during the epiret3 prospective clinical trial. *Invest Ophthalmol Vis Sci*. 2011.

7. Rizzo JF, 3rd. Update on retinal prosthetic research: The boston retinal implant project. *J Neuroophthalmol*. 2011;31:160-168.

8. Stingl K, Bartz-Schmidt KU, Besch D et al. Artificial vision with wirelessly powered subretinal electronic implant alpha-ims. *Proc Biol Sci*. 2013;280:20130077.

9. Fujikado T, Kamei M, Sakaguchi H et al. Testing of semichronically implanted retinal prosthesis by suprachoroidal-transretinal stimulation in patients with retinitis pigmentosa. *Invest Ophthalmol Vis Sci*. 2011;52:4726-4733.

10. Shivdasani MN, Luu CD, Cicione R et al. Evaluation of stimulus parameters and electrode geometry for an effective suprachoroidal retinal prosthesis. *J Neural Eng*. 2010;7:036008.

11. Chowdhury V, Morley JW, Coroneo MT. Evaluation of extraocular electrodes for a retinal prosthesis using evoked potentials in cat visual cortex. *J Clin Neurosci*. 2005;12:574-579.

448 12. Gerding H. A new approach towards a minimal invasive retina implant. *J Neural Eng*.
449 2007;4:S30-37.
450 13. Humayun MS, Dorn JD, da Cruz L et al. Interim results from the international trial of second
451 sight's visual prosthesis. *Ophthalmology*. 2012;119:779-788.
452 14. Kotecha A, Zhong J, Stewart D, da Cruz L. The argus ii prosthesis facilitates reaching and
453 grasping tasks: A case series. *BMC Ophthalmol*. 2014;14:71.
454 15. da Cruz L, Coley BF, Dorn J et al. The argus ii epiretinal prosthesis system allows letter and
455 word reading and long-term function in patients with profound vision loss. *Br J Ophthalmol*.
456 2013;97:632-636.
457 16. Weiland JD, Humayun MS. Retinal prosthesis. *IEEE Trans Biomed Eng*. 2014;61:1412-1424.
458 17. Bonham BH, Litvak LM. Current focusing and steering: Modeling, physiology, and
459 psychophysics. *Hear Res*. 2008;242:141-153.
460 18. Jepson LH, Hottowy P, Mathieson K et al. Spatially patterned electrical stimulation to
461 enhance resolution of retinal prostheses. *J Neurosci*. 2014;34:4871-4881.
462 19. Shivdasani MN, Fallon JB, Luu CD et al. Visual cortex responses to single- and simultaneous
463 multiple-electrode stimulation of the retina: Implications for retinal prostheses. *Invest*
464 *Ophthalmol Vis Sci*. 2012;53:6291-6300.
465 20. Villalobos J, Nayagam DAX, Allen PJ et al. A wide-field suprachoroidal retinal prosthesis is
466 stable and well tolerated following chronic implantation. *Invest Ophthalmol Vis Sci*. 2013:In
467 Press.
468 21. Cicione R, Shivdasani MN, Fallon JB et al. Visual cortex responses to suprachoroidal
469 electrical stimulation of the retina: Effects of electrode return configuration. *J Neural Eng*.
470 2012;9:036009.

22. John SE, Shivdasani MN, Williams CE et al. Suprachoroidal electrical stimulation: Effects of stimulus pulse parameters on visual cortical responses. *J Neural Eng*. 2013;10:056011.

23. John SE, Shivdasani MN, Leuenberger J et al. An automated system for rapid evaluation of high-density electrode arrays in neural prostheses. *J Neural Eng*. 2011;8:036011.

24. Bierer JA, Middlebrooks JC. Auditory cortical images of cochlear-implant stimuli: Dependence on electrode configuration. *J Neurophysiol*. 2002;87:478-492.

25. Urdan TC. Correlation. In: Statistics in plain english, third edition. New York: Routledge, 2010: 79-92.

26. Firszt JB, Koch DB, Downing M, Litvak L. Current steering creates additional pitch percepts in adult cochlear implant recipients. *Otol Neurotol*. 2007;28:629-636.

27. Kanda H, Morimoto T, Fujikado T, Tano Y, Fukuda Y, Sawai H. Electrophysiological studies of the feasibility of suprachoroidal-transretinal stimulation for artificial vision in normal and rcs rats. *Invest Ophthalmol Vis Sci*. 2004;45:560-566.

28. Berenstein CK, Mens LH, Mulder JJ, Vanpoucke FJ. Current steering and current focusing in cochlear implants: Comparison of monopolar, tripolar, and virtual channel electrode configurations. *Ear Hear*. 2008;29:250-260.

29. Device fitting and psychophysical testing - argus ii retinal prosthesis system device fitting manual. online] 2013. Available at: http://www.accessdata.fda.gov/cdrh_docs/pdf11/h110002c.pdf.

30. Zrenner E, Benav H, Bruckmann A et al. Electronic implants provide continuous stable percepts in blind volunteers only if the image receiver is directly linked to eye movement. *ARVO Meeting Abstracts*. 2010;51:4319.

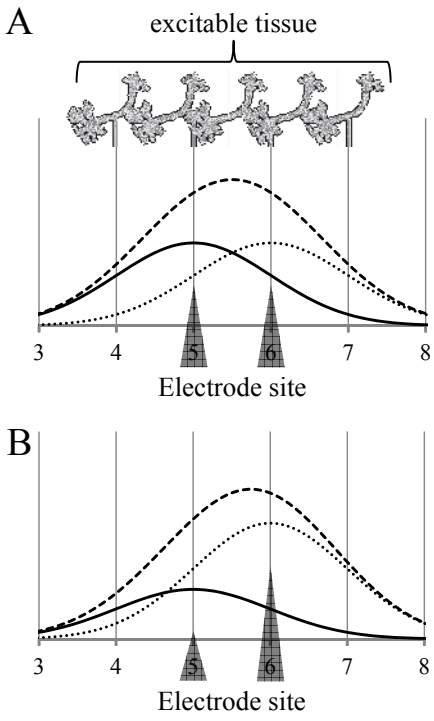
A
excitable tissue
3
4
5
6
7
8
Electrode site
B
3
4
5
6
7
8
Electrode site

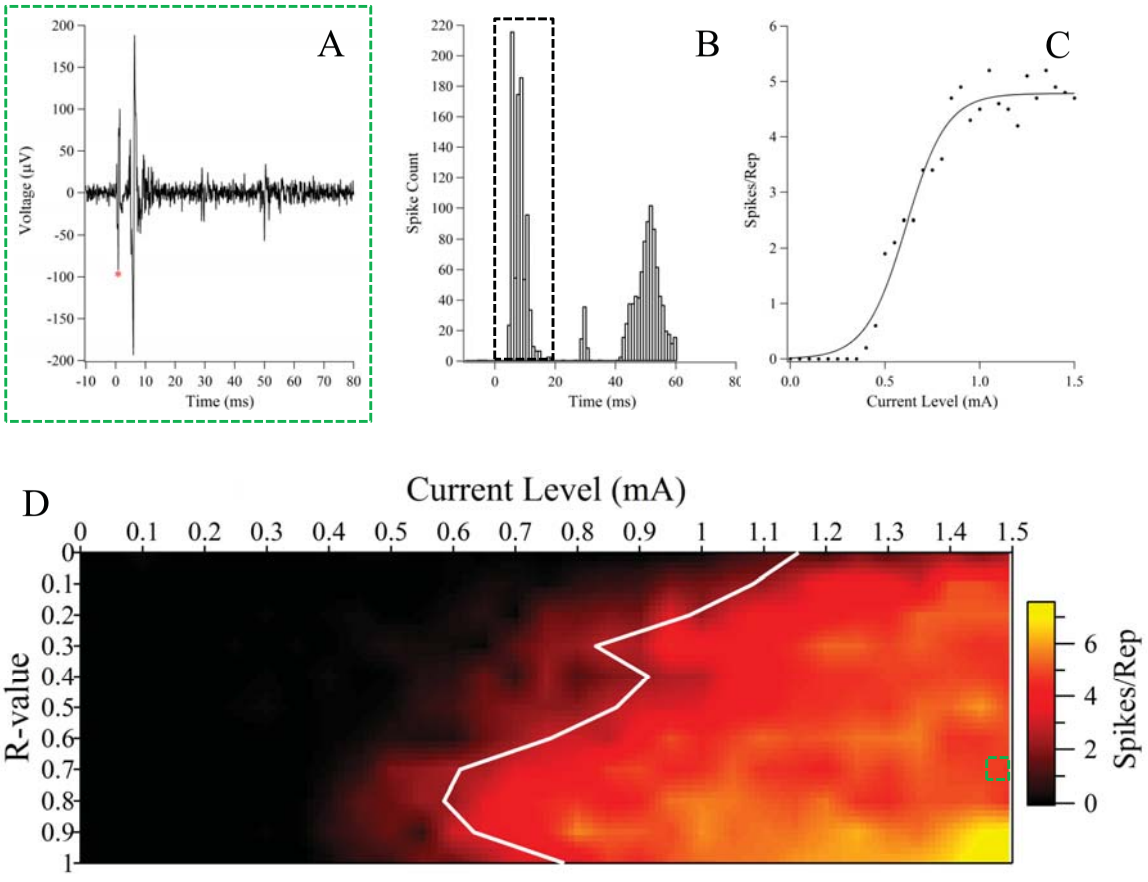
A
Voltage (μV)
Time (ms)
B
Spike Count
Time (ms)
C
Spikes/Rep
Current Level (mA)
D
Current Level (mA)
R-value
Spikes/Rep

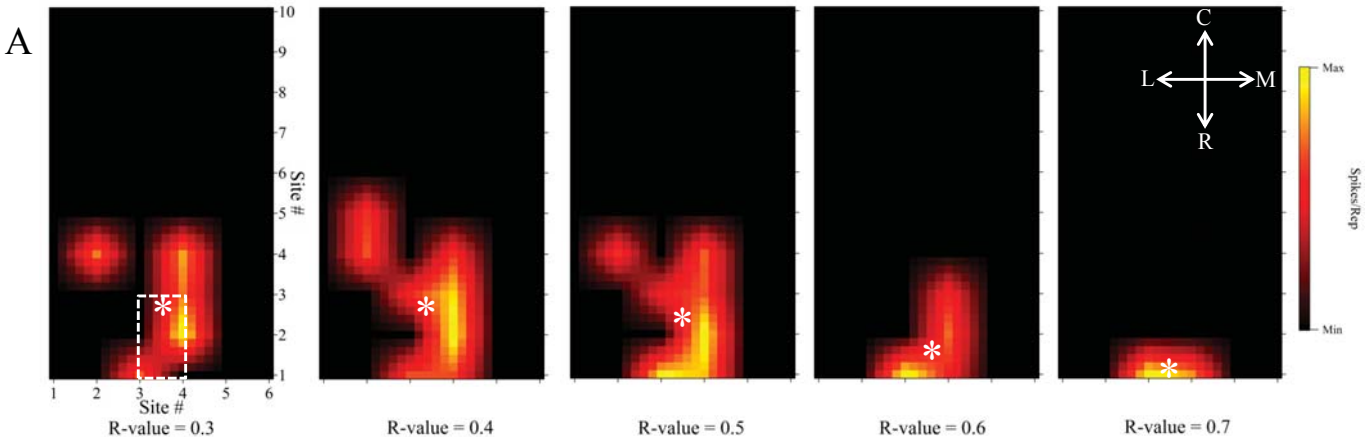
A
C
L
M
R
Max
Min
Spikes/Rep
Site #
R-value = 0.3
R-value = 0.4
R-value = 0.5
R-value = 0.6
R-value = 0.7

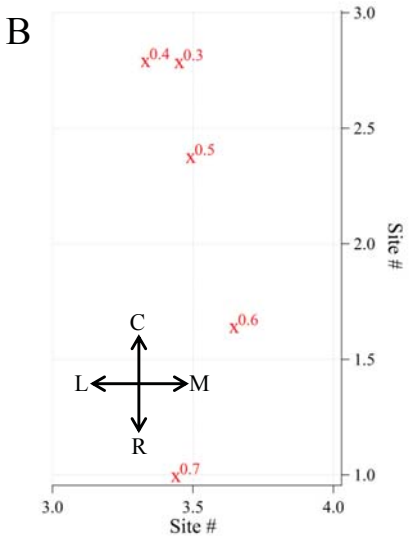
B
x0.4
x0.3
x0.5
x0.6
x0.7
C
L
M
R
Site #
Site #

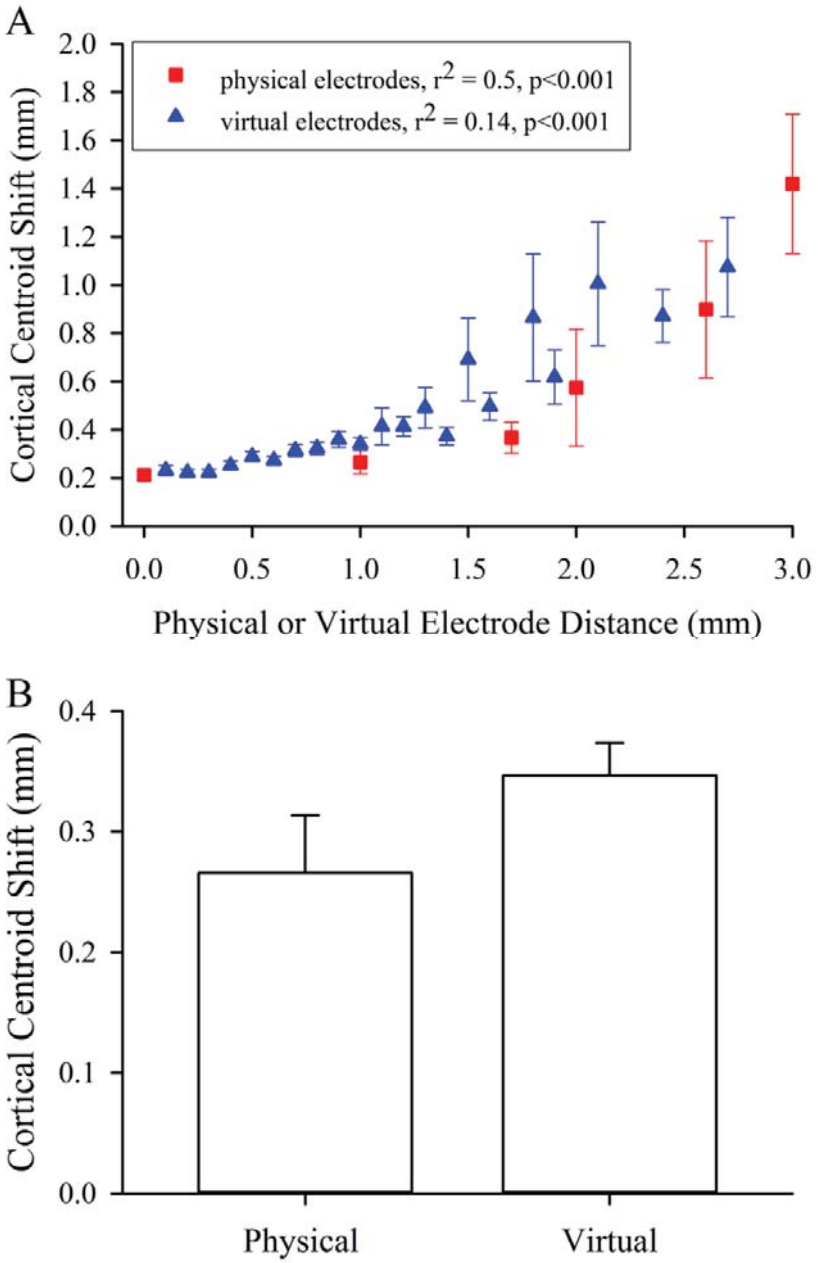
A
physical electrodes, r2 = 0.5, p<0.001
virtual electrodes, r2 = 0.14, p<0.001
Cortical Centroid Shift (mm)
2.0
1.8
1.6
1.4
1.2
1.0
0.8
0.6
0.4
0.2
0.0
0.0
0.5
1.0
1.5
2.0
2.5
3.0
Physical or Virtual Electrode Distance (mm)
B
Cortical Centroid Shift (mm)
0.4
0.3
0.2
0.1
0.0
Physical
Virtual

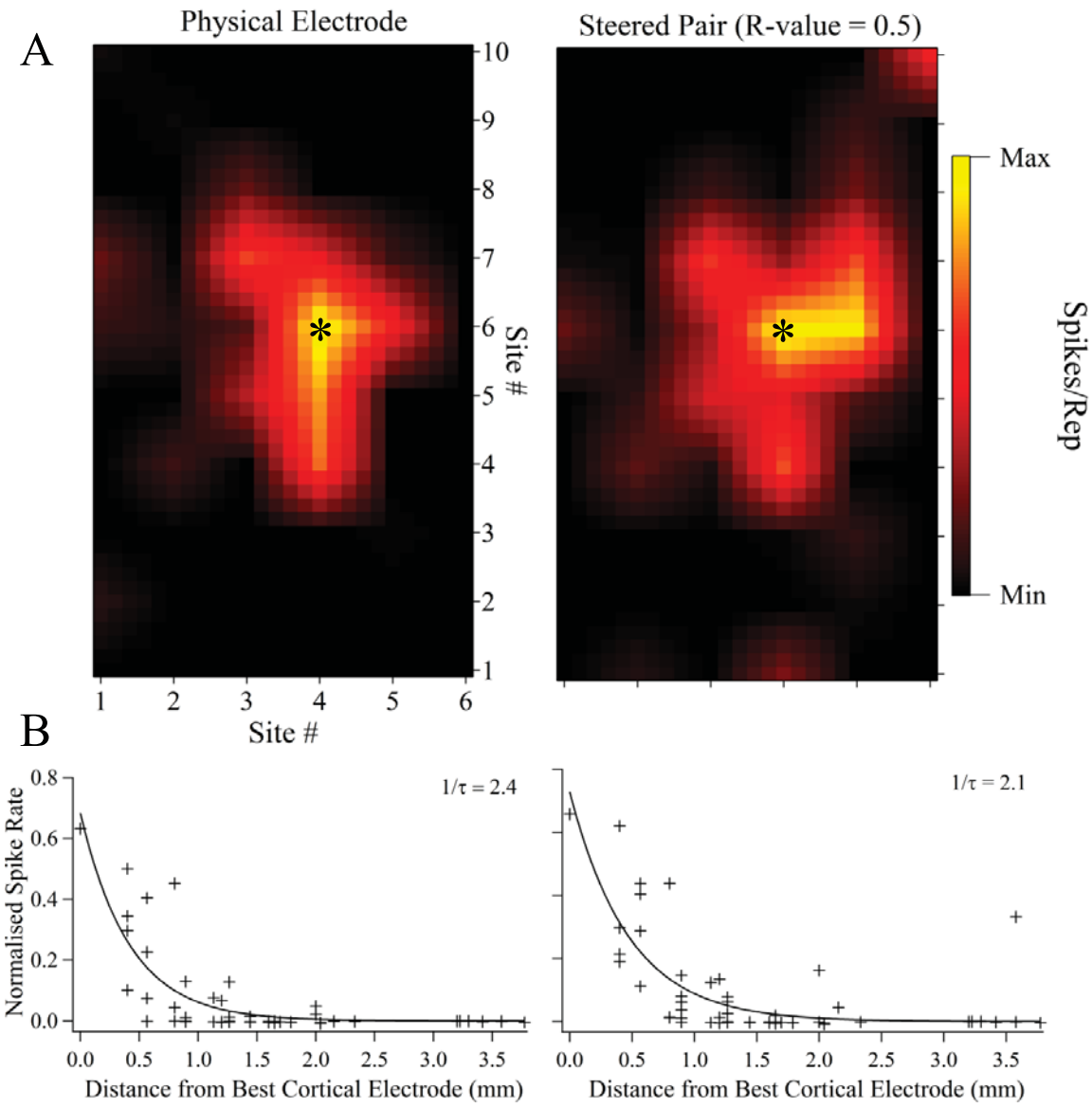
A
Physical Electrode
Steered Pair (R-value = 0.5)
Site #
Site #
Max
Min
Spikes/Rep
B
Normalised Spike Rate
1/τ = 2.4
1/τ = 2.1
Distance from Best Cortical Electrode (mm)
Distance from Best Cortical Electrode (mm)

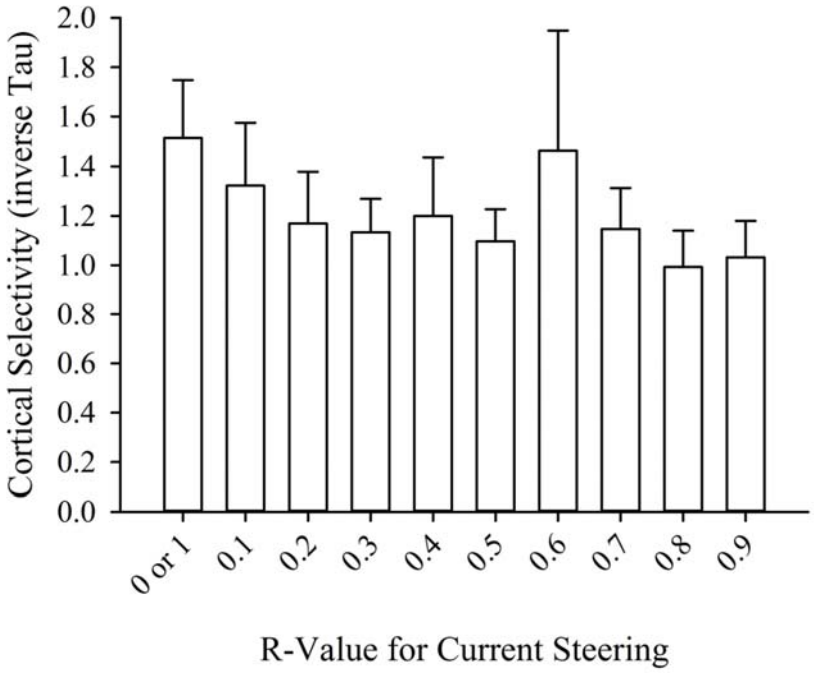
Cortical Selectivity (inverse Tau)
2.0
1.8
1.6
1.4
1.2
1.0
0.8
0.6
0.4
0.2
0.0
0 or 1
0.1
0.2
0.3
0.4
0.5
0.6
0.7
0.8
0.9
R-Value for Current Steering

Author/s:
Dumm, G; Fallon, JB; Williams, CE; Shivdasani, MN

Title:
Virtual Electrodes by Current Steering in Retinal Prostheses

Date:
2014-12-01

Citation:
Dumm, G., Fallon, J. B., Williams, C. E. & Shivdasani, M. N. (2014). Virtual Electrodes by Current Steering in Retinal Prostheses. INVESTIGATIVE OPHTHALMOLOGY & VISUAL SCIENCE, 55 (12), pp.8077-8085. https://doi.org/10.1167/iovs.14-15391.

Persistent Link:
http://hdl.handle.net/11343/43170